Design and end chamfer simulation of PEFP beam line curved dipole magnets

ZHU Ying-Shun(朱应顺)[1,2;1)] YANG Mei(杨梅)[1] ZHANG Zhuo(张卓)[1]
CHEN Wan(陈宛)[1] YIN Bao-Gui(尹宝贵)[1] SHI Cai-Tu(石才土)[1] KANG Wen(康文)[1]

[1] Institute of High Energy Physics, Chinese Academy of Sciences, Beijing 100049, China
[2] Graduate University of Chinese Academy of Sciences, Beijing 100049, China

Abstract: The design, fabrication and field measurement of 11 DC curved dipole magnets for the PEFP Beam Line have been completed. In this paper, a design method for a complex end chamfer using OPERA-3D is proposed. The conventional method for estimating chamfer shape is extended and applied to a curved dipole magnet by a coordinate transformation. Using the interface with CAD software, the complex end chamfer is modeled and fully determined by 3D simulation to meet the field uniformity requirement. The magnetic field measurement results are in good agreement with the simulation. The design considerations, field simulation results, end chamfer development process and measurement results are presented in detail.

Key words: PEFP, dipole magnet, end chamfer

PACS: 29.20.Ej, 41.85.Lc, 07.05.Tp **DOI:** 10.1088/1674-1137/35/7/015

1 Introduction

The Proton Engineering Frontier Project (PEFP) is the first high power proton linac development project in Korea. Its primary goal is to develop a 100 MeV proton linac and supply 20 MeV and 100 MeV proton beams to user groups [1]. The collaboration between the Institute of High Energy Physics (IHEP) and the Korea Atomic Energy Research Institute (KAERI) has been established for the design, manufacture and measurement of the beam line DC dipoles for the PEFP project.

For conventional magnets, the end chamfering (or shimming) is usually performed to improve the three-dimensional field quality. The end chamfer for a dipole magnet is typically used to compensate the sextupole components, and the shape is quadratic. However, it is difficult to model an end chamfer of a complex shape, so normally it is experimentally developed using a prototype with removable poles [2–7]. The end chamfer for a curved magnet is more complex than for a straight magnet, which makes it a challenge, especially for a magnet with small radius and a large bending angle. In designing the PEFP beam line dipoles, the end chamfer is fully determined by 3D simulation. After optimization, the field quality specification is met and a proper end chamfer shape can be provided. Then the end chamfer is fabricated accurately on a CNC machine. This chamfering process replaces the conventional one.

2 Magnet design

2.1 Design requirements and overall consideration

The design requirements of the dipole magnets are listed in Table 1.

For a 20 MeV proton at 0.35 T and a 100 MeV proton at 0.8 T, the bending radius is almost the same. In order to facilitate the magnet design and fabrication, the same magnet operating at two field levels is used both for 20 MeV and 100 MeV protons. All the magnets are designed to have the same cross section but with two different lengths corresponding to different bending angles. The same design method is applied to the two types of magnets.

2.2 Yoke and coil design

Soft iron is used for the magnet core, which is

Received 27 September 2010

1) E-mail: yszhu@ihep.ac.cn

Table 1. Design requirements of the PEFP beam line dipoles.

item	proton energy/MeV	
	20	100
bending angle	25°/45°	25°/45°
quantity	7	4
central magnetic field/T	0.35	0.8
magnet shape	curved magnet with parallel ends	
pole gap height/mm	90	
good field width/mm	±50	
integral field uniformity	0.1%	

curved according to the bending radius of the beam. The C-type structure is chosen to accommodate the vacuum chamber, and the coils can be assembled through the magnet gap. The excitation coils for each pole are made of three pancake-type coils with a total of six layers, and every pancake is cooled by one water circuit. The coils are wound from 16 mm×16 mm square OFHC copper conductor with a 10 mm diameter water-cooling channel.

2.3 Magnetic field analysis without an end chamfer

The magnetic field calculation is performed using OPERA from Cobham Technical Services. The 2D calculation is used to optimize the pole profile and the magnet cross section. Fig. 1 presents the homogeneity of the magnetic field along the transverse axis at two field levels. It is shown that the field uniformity of 0.1% is achieved in 2D simulation.

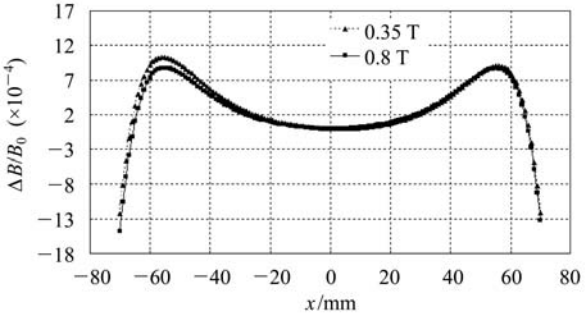

Fig. 1. The 2D transverse field homogeneity.

In the following sections, the 45° magnet is taken as an example to illustrate the field quality optimization process. Firstly, the three-dimensional magnetic performance is investigated before the end chamfering using OPERA-3D/TOSCA. The integral field is obtained by integrating the magnetic field along the ideal beam path, and its distribution in the median plane is shown in Fig. 2.

The maximum field error in the good field region is about 0.7%, which significantly exceeds the requirement. Multipole coefficients are extracted from the

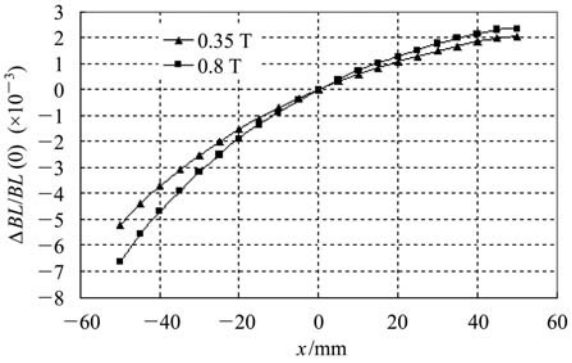

Fig. 2. The transverse distribution of integral field without an end chamfer.

integral field distribution by polynomial fitting:

$$\frac{\Delta BL}{BL(0)} = \sum_{n\geqslant 2} b_n \left(\frac{x}{x_0}\right)^{(n-1)}. \qquad (1)$$

where x_0 is the half width of the good field region, and b_n is the normalized multipole field content compared with the central integral dipole field (see Table 2).

Table 2. Multipole coefficients before end chamfering.

n	b_n @0.35 T	b_n @0.8 T
2	0.0032	0.0039
3	−0.0016	−0.002
4	0.0004	0.0005
5	0.0005	0.0003
6	0.00002	0.00006

3 End chamfer development

3.1 Baseline chamfer shape

First of all, a baseline end chamfer shape is generated according to the 3D simulation result of the unchamfered model. There are two methods to estimate the end chamfer shape: one is the effective length method [6–8], another is the harmonic end chamfer analysis method [9, 10]. The latter method is used here because it can provide more useful guidance not only in the pole end chamfer process, but also in the pole profile design.

Table 2 indicates that it is sufficient to reduce the quadrupole field, sextupole field and octupole field together to get the required field quality. According to the harmonic analysis method, the ideal chamfer curves for compensating the three multipole fields are shown below [9]:

$$\Delta l_2 = -b_2\frac{L}{2}\frac{x}{x_0}, \tag{2}$$

$$\Delta l_3 = -b_3\frac{L}{2}\frac{3x^2-y_0^2}{3x_0^2}, \tag{3}$$

$$\Delta l_4 = -b_4\frac{L}{2}\frac{x^3-xy_0^2}{x_0^3}. \tag{4}$$

where Δl_2, Δl_3, Δl_4 are the chamfer lengths at transverse position x for the quadrupole field, sextupole field and octupole field, respectively. y_0 denotes the half pole gap and L represents the magnetic length. The positive value of the chamfer length means additional iron is needed (end shim), while the negative value means that the iron needs to be removed (end chamfer). The negative sign before b_n means that the end chamfer will produce a multipole field that is exactly opposite to the existing large multipole field. In theory, a combination of Eqs. (2), (3), (4) can reduce the quadrupole field, sextupole field and octupole field simultaneously. However, the actual curve of the total chamfer depth is expressed as follows:

$$d = \alpha(\Delta l_{2\mathrm{N}} + \Delta l_{3\mathrm{N}} + \Delta l_{4\mathrm{N}}) - l_{\max}. \tag{5}$$

where α is the scaling factor reflecting the chamfer efficiency determined by the chamfer angle. The commonly used 45° is adopted in chamfering and an initial value of 2 is set for the scaling factor. The minus sign before $l_{\max}$ in Eq. (5) implies that the chamfer curve is moved down to make d negative at all transverse positions, i.e., the iron is removed and no iron should be added.

The chamfer width is also an important parameter in the chamfering process. According to the harmonic end chamfer analysis, the width of the end chamfer should be larger than the zero chamfer positions of each multipole field [9]. For example, the largest zero chamfer position of the octupole field along x-axis is equal to half the pole gap.

3.2 Coordinate transformation and chamfer optimization

For the curved magnet, the magnetic field is integrated along the beam orbit, so the chamfer depth is also "measured" along the curved beam path. The chamfer curve expressed in this way is hard to model or machine and should be given out in a convenient method. A coordinate transformation from Polar coordinate system to Cartesian coordinate system is introduced. The sketch map of the chamfer in the pole end region is shown in Fig. 3.

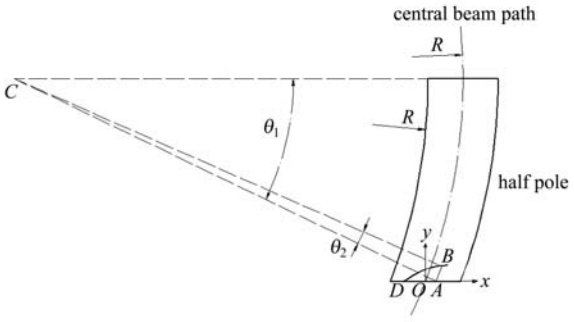

Fig. 3. Sketch of end chamfer.

Point C is the bending center of the central beam path, the curved line DB indicates the chamfer shape and B is an arbitrary point on it. The curved line AB is a section of an arbitrary beam path, whose length is determined by Eq. (5). The origin of the Cartesian coordinate is located at the intersection of the central beam orbit and the pole end edge, and the x, y axes are parallel and perpendicular to the pole edge, respectively. The coordinates of point B are expressed as follows:

$$x_B = x_A + R(\cos(\theta_1-\theta_2)-\cos\theta_1), \tag{6}$$

$$y_B = y_A + R(\sin\theta_1-\sin(\theta_1-\theta_2)), \tag{7}$$

$$\theta_1 = \frac{L_{\mathrm{core}}}{2R},\quad \theta_2 = \frac{d}{R}, \tag{8}$$

in which L_{core} is the magnet core length, and R is the bending radius. Applying formulas (6)–(8), the coordinates of the numerous points on the chamfer curve are obtained in a Cartesian coordinate system.

It should be noted that the chamfer depth on the right hand side is very large. A real chamfer can not be stopped inside the iron, so the chamfer curve should continue and gradually approach zero. A simple inclined straight line is added to the ideal chamfer curve. The pole end edges outside the chamfer region are still rectangular. In order to reduce the magnetic saturation, a 5 mm×45° straight cut is set as the first step of the chamfering process. Hereto the generation of the entire chamfer curve is finished.

According to the chamfer curve, the section of the iron needing to be removed from the pole end is modeled in SOLIDWORKS. Then it is exported as a sat format file and imported into OPERA-3D. Af-

ter Boolean operation, the modeling of the chamfered magnet is completed. The chamfer width and scaling factor need to be adjusted, and the chamfer shape is modified according to the simulation result. After several iterations, the field uniformity is achieved and the suitable end chamfer curve can be obtained. The machining of the pole end region is processed in accordance with the chamfer curve on a CNC machine. The chamfered pole end in 3D simulation for 45° dipoles is illustrated in Fig. 4.

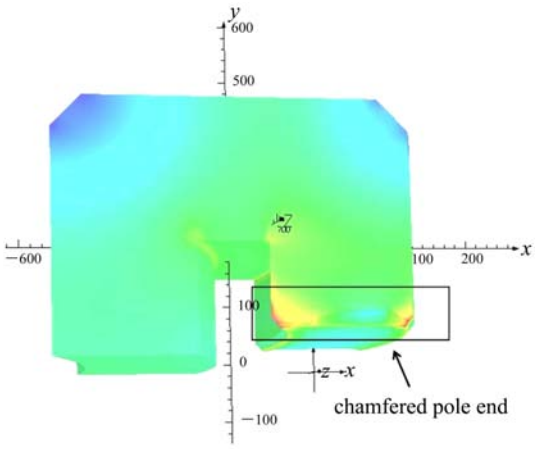

Fig. 4. The chamfered pole end in OPERA-3D simulation.

4 Comparison of the simulation and measurement results

4.1 Hall probe system measurement result

The fabrication of the first two 45° magnets was finished in March 2009, and the magnetic field measurement was performed using the Hall probe system.

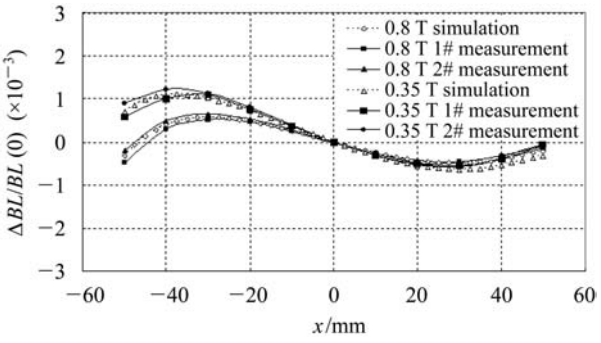

Fig. 5. Comparison of the simulation and Hall probe measurement results.

In order to verify the accuracy of the 3D calculation and take account of the possible fabrication error and uncertainness in material property, firstly a conservative method of using removable pole ends was adopted. After the machining of the end chamfer determined by the 3D simulation, the field was measured along the beam path. The comparison of the measured and simulated integral field distribution is presented in Fig. 5, where the pole centerline corresponds to x=0.

It is shown that the measurement result agrees well with the simulation. The required field uniformity is met and no further chamfer development is necessary.

4.2 Translating long coil measurement result

It was decided that no removable pole end was used for the rest nine magnets. Although the end chamfer curve for the 25° dipole is different from the 45° dipole, it is directly manufactured according to the 3D simulation. The magnetic measurement is done by the translating long coil system with a newly fabricated curved measurement coil as shown in Fig. 6. The measurement of the five 45° magnets repeats the result of the first two magnets well and the measurement result of the four 25° magnets is presented in Fig. 7.

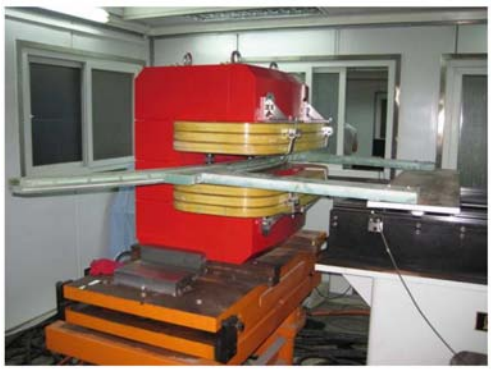

Fig. 6. Translating long coil measurement.

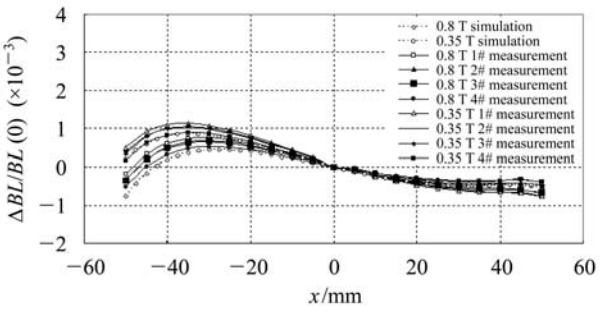

Fig. 7. Comparison of the simulated and measured results for 25° magnets.

Figure 7 shows that the peak-to-peak field uniformity of each magnet is within ±0.1%, which satisfies the specification, and the small deviation of the inte-

gral field distributions of the four magnets is acceptable. Again, good agreement between the simulated and measured results is achieved. All the field measurement data had been checked by the PEFP side, and the magnets were delivered on schedule to Korea in October 2009.

5 Conclusion

All the PEFP beam line DC dipoles are designed, manufactured and measured successfully. A proper end chamfer for the curved magnet is developed and fully determined by 3D simulation to meet the field uniformity requirement. The validity of the end chamfer method for the curved magnet using OPERA-3D is confirmed by the field measurement result. This method can be applied to similar dipole magnets.

The authors would like to thank Prof. YIN Zhao-Sheng for useful discussion and acknowledge all colleagues of the Magnet Group.

References

1 JANG J, Cho Y, Choi B et al. The Korean Proton Engineering Frontier Project. In: Proceedings of Hadron Beam 2008, Nashville, USA. 422
2 CHANG C H, LIU H C, Hwang G J. Design and Performance of the Dipole Magnet for the SRRC Storage Ring. In: Proceedings of PAC 1993, Washington, USA. 2886
3 Barale P, LI N, Osborn J et al. Optimization of the PEP-Ⅱ Low-Energy Ring Dipoles. In: Proceedings of PAC 1997, Vancouver, Canada. 3312
4 Werner M, Vrankovic V, George D C. IEEE Trans. Appl. Supercond., 2000, **10**(1): 248
5 YAO Cheng-Gui, ZHOU Qiao-Gen, CAO Zan et al. Journal of University of Science and Technology of China, 2001, **31** (2): 202 (in Chinese)
6 CHEN W, SHI C T, YIN B G et al. End Chamfer Study and Field Measurements of the BEPC Ⅱ Dipoles. In: Proceedings of PAC 2005, Knoxville, USA. 919
7 Tanabe J. Iron Dominated Electromagnets: Design, Fabrication, Assembly and Measurements. World Scientific Pub Co Inc, 2005. 252
8 Pont M, Boter E, Lopes M et al. Magnets for the Storage Ring ALBA. In: Proceedings of EPAC 2006, Edinburgh, Scotland. 2562
9 ZHAO Ji-Jiu, YIN Zhao-Sheng. Particle Accelerator Technology. Beijing: Higher Education Press, 2006. 51 (in Chinese)
10 YIN Z S, WU Y Z, ZHANG J F et al. Nucl. Instrum. Methods Phys. Res. A, 2007, **573** (3): 323